A Fast Multi-Level GFSK Matched Filter Receiver

Charles Tibenderana and Stephan Weiss
School of Electronics & Computer Science, University of Southampton, UK

Abstract

Near optimal reception of a multilevel Gaussian frequency shift keying symbol can be achieved using a matched filter bank (MFB) receiver, which will require M^{K+L-1} filters for M modulation levels, a K-symbol observation interval, and a Gaussian filter with an L-symbol support length. This is prohibitive for most applications for the large values of K necessary to ensure best performance. In this paper we present a recursive algorithm that eliminates redundancy in providing the matched filter outputs by use of a smaller set of 1-symbol long intermediate filters, followed by an iterative process to propagate phase gained over K successive single symbol stages. If exemplarily operated in a Bluetooth receiver, the computational cost can be reduced by two orders of magnitude. Additionally we demonstrate that the intermediate filter outputs provide a means to detect carrier frequency and modulation index offsets, which can be corrected by iteratively recomputing the coefficients of the intermediate filter bank.

1 Introduction

Gaussian frequency shift keying (GFSK) is a bandwidth preserving digital modulation technique, which has been used for low-cost transmission standards such as Bluetooth [1]. Optimum detection of a sequence of GFSK modulated symbols can be achieved by a Viterbi receiver [2]. However, the Viterbi detector requires a rational and precisely known modulation index, which in e.g. Bluetooth is permitted to vary such that performance is degraded [3]. Relatively simple GFSK reception techniques such as FM-AM conversion, phase-shift discrimination and zero-crossing detection [4] yield only modest bit error ratio (BER) performance [5]. Therefore, a high performance receiver based on matched filtering of GFSK signals is considered here [6, 7].

For M-level GFSK (M-GFSK), an observation interval of K symbol periods and N samples per symbol will require M^{K+L-1} filters of length KN, where L is the support length of the Gaussian filter in symbol periods. This is a prohibitively large filter bank for high values of K necessary to ensure best performance. Thus, as an extension of our work in [8], which addressed binary GFSK, in this paper we propose a low-cost realisation of the MFB that eliminates redundancy in providing the matched filter outputs by use of a smaller set of 1-symbol long intermediate filters, followed by an iterative process to propagate phase gained over K successive single symbol stages.

Furthermore, since multipath propagation, carrier frequency and modulation index offsets pose potential problems to Bluetooth transmissions, in the past we have addressed equalisation issues [9], and carrier frequency correction via a novel stochastic gradient descent algorithm [8]. In this paper we demonstrate that the intermediate filter outputs provide a means to detect carrier frequency and modulation index offsets, which can be corrected by iteratively recomputing the coefficients of the intermediate filter bank.

Hence, this paper will, based on a signal model developed in Sec. 2, present a brief review of the standard MFB receiver in Sec. 3, before a derivation of the lower cost MFB receiver for M-GFSK signals in Sec. 4. Sec. 5 addresses synchronisation of carrier frequency and modulation index, while Sec. 6 discusses simulation results. We conclude in Sec. 7.

2 Signal Model

M-GFSK modulation requires that groups of N_b data bits are mapped onto multilevel symbols, $p[k]$. Each symbol can have one of M amplitude levels, symmetrically distributed above and below zero, such that $M = 2^{N_b}$, whereby the mapping from bit to symbol stream is accomplished via Gray coding [10]. The resulting symbol sequence is expanded by a factor of N and passed through a Gaussian filter with impulse response $g[n]$ of length LN [10], thus having a support of L symbol periods and yielding

$$\omega[n] = 2\pi h \sum_{k=-\infty}^{\infty} p[k] g[n - kN] \quad , \tag{1}$$

where h is the modulation index. The phase of the discrete quadrature baseband transmitted signal,

$$s[n] = e^{j\theta[n]} = \exp\{j \sum_{\nu=-\infty}^{n} \omega[\nu]\} = \prod_{\nu=-\infty}^{n} e^{j\omega[\nu]} \quad , \tag{2}$$

is determined as the cumulative sum over all previous phase values $\omega[n]$ in (1).

The Gaussian filter introduces intersymbol interference, with each symbol significantly affecting $(L-1)/2$ adjacent symbols on each side. Consequently, instantaneous frequency waveforms $\omega[n]$, portrayed in Fig. 1, could form an eye, with M^L possibilities per symbol period. Fig. 1 also illustrates that the number of authentic phase trajectories during the kth symbol period is M^k.

We assume that the received signal, $r[n]$, has been subject to an attenuation by a complex gain A, and is contaminated by additive white Gaussian noise (AWGN) $v[n]$, that is uncorrelated with the transmitted signal $s[n]$, so that

$$r[n] = A \cdot s[n] + v[n] \quad . \tag{3}$$

The channel model implied in (3) is narrowband. If time-dispersiveness of the channel was an issue, then blind equalisation [9] can restore the assumed form (3) in the receiver.

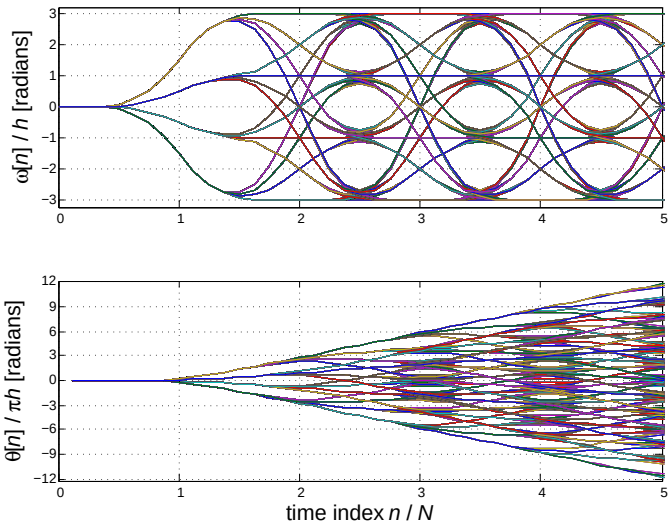

Fig. 1. Instantaneous frequency (top) and phase (bottom) trees for a GFSK modulated signal, with $M = 4$, and $K_{BT} = 0.5$ ($L = 3$).

3 Matched Filter Bank Receiver

A standard MFB receiver, which achieves near-optimum non-coherent estimation of a continuous phase modulated symbol in AWGN is discussed in [6, 7]. The method is based on a filter bank containing all legitimate transmitted sequences $s[n]$ over a duration of K symbol periods. Over this observation interval, due to the support length of the Gaussian filter, M^{K+L-1} possible sequences exist if we neglect the initial phase shift. The filter with the largest output determines the received signal, and assuming K is odd, the symbol at the center of the modulating symbol sequence, responsible for producing the received signal, is chosen as the detected symbol. A Gray decoder maps the estimated symbol level onto a received N_b-bit vector $\hat{\mathbf{b}}[k]$.

The detector selects the largest magnitude value from the matched filter bank output, determining the detected symbol $\hat{p}[k]$ as

$$\hat{p}[k] = \arg\max_i \left| \sum_{n=0}^{KN-1} r[kN-n] \cdot s^*_{i,j}[-n] \right| \quad , \tag{4}$$

where $s^*_{i,j}[-n]$ are the M^{K+L-1} K-symbols long matched filter responses with initial phase of 0, and $i \in \{\pm 1, \pm 3, \pm 5, \ldots, \pm(M-1)\}$ indicates the value of the middle symbol, while $j = 0(1)M^{K+L-2}$ indexes the possible transmitted waveforms with i at the center of their modulating symbol sequence. Note that the detector imposes a delay such that ideally $\hat{p}[k] = p[k - \frac{K+1}{2}]$. The performance of this receiver improves with increase in K. However, despite its performance merits, the computational complexity accrues to

$$C_{\text{standard}} = 2\ NKM^{K+L-1} \tag{5}$$

real valued multiply accumulates (MACs). The cost in (5) considers the fact that the possible sequences $s_{i,j}[n]$ consist of complex conjugate pairs, and that a complex valued operation accounts for 4 real valued ones. Nevertheless, the complexity in (5) is prohibitively large for implementation. Therefore, in the following we seek a low complexity implementation of this receiver.

4 Low-Complexity Receiver

We will first inspect the matched filter responses in Sec. 4.1, and thereafter develop a recursive scheme for their representation in Sec. 4.2, leading to an analysis of its complexity in Sec. 4.3.

4.1 Received Signals

Let us assume that K-symbol periods of the received signal $r[n]$ are held in a tap delay line (TDL) vector $\mathbf{r}_k$, synchronised with the kth symbol to be the most recent datum,

$$\mathbf{r}_k = \begin{bmatrix} \tilde{\mathbf{r}}_k \\ \tilde{\mathbf{r}}_{k-1} \\ \vdots \\ \tilde{\mathbf{r}}_{k-K+1} \end{bmatrix} = A \cdot \mathbf{s}_k + \mathbf{v}_k = A \underbrace{\begin{bmatrix} \tilde{\mathbf{s}}_k \\ \tilde{\mathbf{s}}_{k-1} \\ \vdots \\ \tilde{\mathbf{s}}_{k-K+1} \end{bmatrix}}_{\mathbf{s}_k} + \mathbf{v}_k \quad ,$$

where $\mathbf{v}_k \in \mathbb{C}^{NK}$ holds the noise samples. The vector $\tilde{\mathbf{s}}_k$ is defined as

$$\tilde{\mathbf{s}}_k = [s[kN] \;\; s[kN-1] \;\; \ldots \;\; s[(k-1)N+1]]^{\mathrm{T}} \quad ,$$

and $\tilde{\mathbf{r}}_k$ is defined analogously. According to (2), $\tilde{\mathbf{s}}_k$, holding N samples within a symbol period, can be expanded as

$$\tilde{\mathbf{s}}_k = \underbrace{\begin{bmatrix} \prod_{\nu=(k-1)N+1}^{kN} e^{j\omega[\nu]} \\ \prod_{\nu=(k-1)N+1}^{kN-1} e^{j\omega[\nu]} \\ \vdots \\ e^{j\omega[(k-1)N+1]} \end{bmatrix}}_{\mathbf{u}_k} \cdot \prod_{\nu=-\infty}^{(k-1)N} e^{j\omega[\nu]} \tag{6}$$

whereby for the samples in $\mathbf{u}_k$ the instantaneous frequency is only accumulated from the start of the kth symbol period. Inserting (6) into $\mathbf{s}_k$ yields

$$\mathbf{s}_k = \begin{bmatrix} \mathbf{u}_k & \cdot e^{j(\theta_{k-K+1}+\cdots+\theta_{k-2}+\theta_{k-1})} \\ \mathbf{u}_{k-1} & \cdot e^{j(\theta_{k-K+1}+\cdots+\theta_{k-2})} \\ \vdots & \\ \mathbf{u}_{k-K+2} & \cdot e^{j\theta_{k-K+1}} \\ \mathbf{u}_{k-K+1} & \cdot 1 \end{bmatrix} \cdot e^{j\alpha} \tag{7}$$

with

$$\theta_k = \sum_{\nu=(k-1)N+1}^{kN} w[\nu] \quad \text{and} \quad \alpha = \sum_{\nu=-\infty}^{(k-K)N} w[\nu].$$

Firstly, note that each vector $\mathbf{u}_m$ can take on the shape of M^L different waveforms, whereby L is the support length of the Gaussian window in bit periods. Secondly, observe that a phase correction term $e^{j\theta_k}$ contains the instantaneous frequency values accumulated over the kth symbol period, which is held in the top element of $\mathbf{u}_k$ in (6) and is applied to all subsequent bit periods. The initial phase of $s[n]$ entering the TDL is α.

4.2 Recursive Matched Filter Formulation

The matched filter responses $s^*_{i,j}[-n]$ are designed from the transmitted signal $s[n]$ in (2). Utilising the previous observation that $\mathbf{u}_k$ only takes on M^L basic waveforms independent of k, we will construct a matched receiver in steps. It is important to note that the following derivation is independent of the mapping system used to encode N_b data bits onto a specific symbol.

Case $K = 1$. Consider a matched filter for $K = 1$ covering the kth symbol period. The M^L matched filter outputs are given by

$$\mathbf{y}_k^{(1)} = \mathbf{W}^{(1)}\ \tilde{\mathbf{r}}_k \quad , \tag{8}$$

with $\mathbf{W}^{(1)} \in \mathbb{C}^{M^L \times N}$ containing all legitimate complex conjugated and time reversed waveforms in its rows. The superscript $^{(1)}$ indicates that only a single symbol period $K = 1$ is observed. The first column of $\mathbf{W}^{(1)}$, denoted by $\mathbf{w}$, holds the M^L authentic values for $e^{-j\theta_k}$ from (7). We assume that the first row of $\mathbf{W}^{(1)}$ contains the matched filter coefficients for N_b bits at the center of LN_b total bits, all of value 0, binary coded decimally down to the last row with LN_b bits of value 1.

Case $K = 2$. Expanding to $K = 2$, we can denote

$$\mathbf{y}_k^{(2)} \;=\; \mathbf{W}^{(2)} \begin{bmatrix} \tilde{\mathbf{r}}_k \\ \tilde{\mathbf{r}}_{k-1} \end{bmatrix} \quad ,$$

with $\mathbf{W}^{(2)} \in \mathbb{C}^{M^{L+1} \times 2N}$ consisting of all possible M^{L+1} complex conjugated and time reversed transmitted waveforms in its rows. Therefore note that in constructing the M^{L+1} matched filter responses in $\mathbf{W}^{(2)}$, only one extra symbol needs to be considered compared to the responses in $\mathbf{W}^{(1)}$.

Example. For $L = 3$ and $M = 2$ ($N_b = 1$), the rows in $\mathbf{W}^{(1)}$ should contain the central N samples of the responses to the bit sequences {0,0,0} to {1,1,1}, while $\mathbf{W}^{(2)}$ would cater for an additional symbol, hence covering the middle $2N$ samples of bit combinations {0,0,0,0} to {1,1,1,1}. Thus, for each possible sequence contained in $\mathbf{W}^{(1)}$, two new possibilities arise in $\mathbf{W}^{(2)}$, and so on for higher values of K.

Thus, M^L outputs of filter bank $\mathbf{W}^{(1)}$ from the previous symbol period can be used with its current results to compute the M^{L+1} outputs of $\mathbf{W}^{(2)}$, enabling us to write

$$\begin{aligned} \mathbf{y}_k^{(2)} \;&=\; \mathbf{D}^{(2)}\ \mathbf{A}^{(2)}\ \mathbf{W}^{(1)}\ \tilde{\mathbf{r}}_k \;+\; \mathbf{M}^{(2)}\ \mathbf{W}^{(1)}\ \tilde{\mathbf{r}}_{k-1} \\ &=\; \mathbf{D}^{(2)}\ \mathbf{A}^{(2)}\ \mathbf{y}_k^{(1)} \;+\; \mathbf{M}^{(2)}\ \mathbf{y}_{k-1}^{(1)} \end{aligned}$$

whereby $\mathbf{y}_{k-1}^{(1)}$ are the single symbol matched filter outputs for the $(k-1)$st symbol. The matrix $\mathbf{A}^{(2)}$,

$$\mathbf{A}^{(2)} = \text{blockdiag}\Big\{\begin{bmatrix} 1 & \dots & 1 \end{bmatrix}^T\Big\} \in \mathbb{Z}^{M^{L+1}\times M^L} \quad ,$$

produces $(M-1)$ extra copies of each response in $\mathbf{W}^{(1)}$, while

$$\mathbf{D}^{(2)} = \begin{bmatrix} \text{diag}\{\mathbf{w}\} & & \mathbf{0} \\ & \ddots & \\ \mathbf{0} & & \text{diag}\{\mathbf{w}\} \end{bmatrix} \in \mathbb{C}^{M^{L+1}\times M^{L+1}}$$

applies the phase correction term $e^{-j\theta_k}$, and the matrix

$$\mathbf{M}^{(2)} = \begin{bmatrix} \mathbf{I}_{M^L} & \dots & \mathbf{I}_{M^L} \end{bmatrix}^T \in \mathbb{Z}^{M^{L+1}\times M^L}$$

is assigning the expansion by the extra symbol considered when proceeding from $K=1$ to $K=2$, whereby $\mathbf{I}_{M^L}$ is an $M^L \times M^L$ identity matrix.

Case K arbitrary. Generalising from the previous cases, we formulate recursively for $\mathbf{y}_k^{(K)} \in \mathbb{C}^{M^{K+L-1}}$

$$\mathbf{y}_k^{(K)} = \mathbf{D}^{(K)}\,\mathbf{A}^{(K)}\,\mathbf{y}_k^{(K-1)} \;+\; \mathbf{M}^{(K)}\,\mathbf{y}_{k-K+1}^{(1)} \;,$$

with $\mathbf{y}_{k-K+1}^{(1)}$ according to (8), where

$$\mathbf{M}^{(K)} = \Big[\mathbf{M}^{(K-1)} \;\dots\; \mathbf{M}^{(K-1)}\Big]^T \in \mathbb{Z}^{M^{L+K-1}\times M^L}, \quad (9)$$

with $\mathbf{M}^{(1)} = \mathbf{I}_{M^L}$,

$$\mathbf{A}^{(K)} = \begin{bmatrix} \mathbf{A}^{(K-1)} & & \mathbf{0} \\ & \ddots & \\ \mathbf{0} & & \mathbf{A}^{(K-1)} \end{bmatrix} \in \mathbb{Z}^{M^{L+K-1}\times M^{L+K-2}}, \quad (10)$$

with

$$\mathbf{A}^{(1)} = \text{blockdiag}\{[\underbrace{1 \;\dots\; 1}_{M}]^{\mathrm{T}}\} \in \mathbb{Z}^{M^L\times M^{L-1}} \quad ,$$

and

$$\mathbf{D}^{(K)} = \begin{bmatrix} \mathbf{D}^{(K-1)} & & \mathbf{0} \\ & \ddots & \\ \mathbf{0} & & \mathbf{D}^{(K-1)} \end{bmatrix} \in \mathbb{Z}^{M^{L+K-1}\times M^{L+K-1}}, \quad (11)$$

with $\mathbf{D}^{(1)}$= diag$\{\mathbf{w}\}$.

This form of the matched filter bank receiver is depicted by the flow graph in Fig. 2. A detector similar to (4), selecting the index of the largest element, would operate on $\mathbf{y}_k^{(K)}$ to determine the detected symbol, from which in turn the detected bit sequence can be retrieved by Gray decoding.

4.3 Computational Complexity

Inspecting the operations in Fig. 2, per symbol period M^L matched filter operations of length N have to be performed. The matrices $\mathbf{M}^{(k)}$ and $\mathbf{A}^{(k)}$ only performing indexing, the only arithmetic operations required are multiplications with the diagonal elements of the phase correction matrices $\mathbf{D}^{(K)}$, yielding a total of

$$C_{\text{efficient}} = 4M^L N + 4\sum_{k=1}^{K-1} M^{L+k} \approx 4M^L(N + M^{K-1}) \quad (12)$$

MACs.

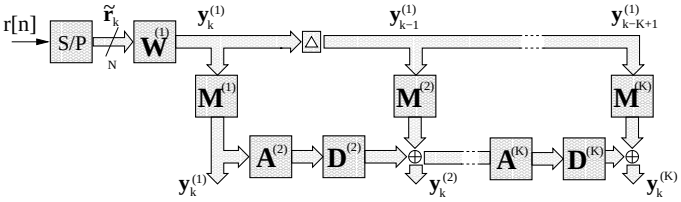

Fig. 2. Low-complexity implementation of a MFB receiver for GFSK. The received signal $r[n]$ is passed through a serial/parallel converter and a filter bank $\mathbf{W}^{(1)}$ with a single symbol (representing N_b bits) duration. Processed over K stages, the matched filter bank outputs are contained in $\mathbf{y}_k^{(K)}$.

5 Synchronisation

In this section we assume a mismatch such that the carrier frequency and modulation index adopted by the transmitter and receiver are Ω and h, and $\hat{\Omega}$ and $\hat{h}$ respectively, and we modify the received signal in (3) to

$$r[n] = s[n]e^{j\Omega n} + v[n] \quad , \quad (13)$$

to cater for a non-zero baseband carrier frequency. Discussions here highlight our work in [11], and though limited to binary GFSK, may be extended to M-GFSK.

5.1 Carrier Frequency

By excluding the noise term in (13), such that

$$r[n] = s[n]e^{j\Omega n} \quad ,$$

it is obvious that $\angle\mathcal{E}\{r[n]\} \propto \Omega$, and therefore the offset $\Delta\Omega = \Omega - \hat{\Omega}$ causes the difference in phase trajectories computed by the transmitter and receiver across a symbol period to be $\Delta\Omega\cdot\binom{N+1}{2}$ if we assume zero initial phase. Thus, the phase term

$$\eta = \angle\mathcal{E}\left\{\left(y_{k-(K-1)/2}^{(1)}\cdot\left(y_{k-(K-3)/2}^{(1)}\right)^*\right)\right\} \propto \Delta\Omega \quad (14)$$

can be verified to be proportional to the mismatch in carrier frequency $\Delta\Omega$. In (14), the quantity $y_k^{(1)}$ refers to the element of $\mathbf{y}_k^{(1)}$ in Fig. 2, associated with the correct symbol sequence leading to the detection of the middle symbol $p[k-\frac{K+1}{2}]$. The complex conjugate term in (14) ensures that the phase is measured relative to zero.

Due to (14), the receiver carrier frequency estimate $\hat{\Omega}$ can be adjusted by

$$\hat{\Omega}[k+1] = \hat{\Omega}[k] + \mu_\Omega\cdot\hat{\eta}[k] \quad ,$$

where $\hat{\eta}[k]$ is an instantaneous estimate of the term in (14) based on a single symbol period,

$$\hat{\eta}[k] = \angle\left\{y_{k-(K-1)/2}^{(1)}\cdot\left(y_{k-(K-3)/2}^{(1)}\right)^*\right\} \quad . \quad (15)$$

Note that in (15), the element $y_k^{(1)}$ is based on the estimated bit sequence rather than the true quantities assumed in (14). Since $y_k^{(1)}$ is available from the proposed low-cost MFB, the only additional complexity arises from $2^L N$ MACs for modifying $\mathbf{W}^{(1)}$ and consequently $\mathbf{D}^{(k)}$.

5.2 Modulation Index

Observation of (1) and (2) reveals that $|\angle\{s[n]\}| \propto h$. Since both the transmitted signal and $\mathbf{W}^{(1)}$ are derived from (1) and (2), if $K_{BT} = \infty$, the maximum phase change in $s[n]$ due to a bipolar symbol $p[k]$ is $\pi h p[k]$, and consequently, assuming zero initial phase and $\Delta\Omega = 0$, the output of a matching intermediate

filter will be $e^{j\pi(h-\hat{h})p[k]}$. This idea can be generalised via the phase term

$$\chi = \angle\mathcal{E}\left\{\left(y^{(1)}_{k-(K-1)/2}\cdot(y^{(1)}_{k-(K-3)/2})^*\right)\cdot p\left[k-\frac{K+1}{2}\right]\right\}\propto\Delta h \quad , \tag{16}$$

which can be verified to be proportional to the mismatch in modulation index $\Delta h = h-\hat{h}$. Analogous to Sec. 5.1, in (16), the quantity $y^{(1)}_k$ refers to the element of $\mathbf{y}^{(1)}_k$ in Fig. 2, associated with the correct symbol sequence leading to the detection of the middle symbol $p[k-\frac{K+1}{2}]$. The complex conjugate term in (16) ensures that the phase is measured relative to zero, while $p[k-\frac{K+1}{2}]$ compensates for the sign change imposed by the middle symbol onto the phase.

To adapt the modulation index estimate $\hat{h}$ and therefore $\mathbf{W}^{(1)}$ and $\mathbf{D}^{(k)}$ in the receiver, we employ an iterative technique

$$\hat{h}[k+1] = \hat{h}[k] + \mu_h\cdot\hat{\chi}[k] \quad , \tag{17}$$

where $\hat{\chi}[k]$ is an instantaneous estimate of the term in (16) based on a single symbol period,

$$\hat{\chi}[k] = \angle\left\{y^{(1)}_{k-(K-1)/2}\cdot(y^{(1)}_{k-(K-3)/2})^*\right\}\cdot\hat{p}[k] \tag{18}$$

Note that in (18), the element $y^{(1)}_k$ is based on the estimated bit sequence and the estimated middle bit $\hat{p}[k]$ rather than the true quantities assumed in (16). The adaptation of $\hat{h}[k]$ according to (17) requires few extra computations since the coefficients in $\mathbf{W}^{(1)}$ and subsequently $\mathbf{D}^{(k)}$ can be adjusted together with the carrier frequency offset estimate at the same time.

6 Simulations and Results

In our simulations Gray coding was according to [12], with $h = 0.35/(M-1)$, $K_{BT} = 0.5$, $L = 3$, $N = 2$ and $\Omega = 0$, so as to model a Bluetooth signal when $M = 2$. Where applicable the maximum offsets permitted by the Bluetooth standard of $\Delta\Omega = \frac{2\pi 75}{N\cdot 1000}$ and $\Delta h = 0.07$ will be adopted [1].

The BER achieved by the more efficient MFB receiver has identical performance to its standard counterpart and is exemplified in Fig. 3, which demonstrates that BER=10^{-3} — the maximum allowed in Bluetooth [1] — is attained at 10.8 dB E_b/N_0 while the best of relatively simple demodulation methods would require 14.8 dB for the same feat [5]. BER reduces for longer K, and selecting larger M degrades BER but increases data rate without additional bandwidth. Fig. 4 illustrates that a Bluetooth link, with maximum permissible values for $\Delta\Omega$ and Δh can be restored by the correction algorithms, thereby saving system collapse or 3 dB respectively.

The analytic complexity evaluation in Tab. 1 shows that the increase in computational cost rises much more rapidly with K, M, and N in the standard MFB than in its efficient realisation. For example when $K = 9$ and $M = N = 2$, cost reduction is 94.4%, when $M = 16$, $K = 5$ and $N = 2$ the gain is 99.9%, and when $N = 32$, $M = 2$ and $K = 5$ the complexity decrease is 96.9%.

7 Conclusion

Relatively simple wireless standards like Bluetooth, which employ GFSK, will have extra capacity if sharing a hardware platform with a more complex one. We suggest a low-cost MFB as an efficient way to use this extra resource to improve BER. We have demonstrated that additional benefit of our receiver is the ease with which carrier frequency and modulation index offsets, typical in inexpensive systems, can be detected and corrected.

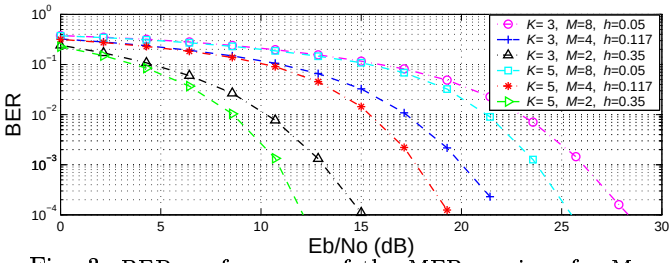

Fig. 3. BER performance of the MFB receiver for M-GFSK signals with $K \in \{3,5\}$, $M \in \{2,4,8\}$, and K_{BT}=0.5 ($L = 3$).

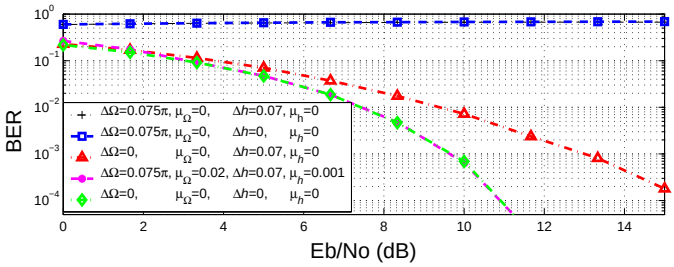

Fig. 4. BER performance improvement due to carrier frequency and modulation index correction algorithms with $K_{BT} = 0.5$, $h = 0.35$, $N = 2$, and $K = 9$.

K (with $M=2$ & $N=2$)	3	5	7	9
C_{standard}/[MAC]	3.8E2	2.6E3	1.4E4	7.4E4
$C_{\text{efficient}}$/[MAC]	1.1E2	3.0E2	1.1E3	4.1E3
M (with $K=5$ & $N=2$)	2	4	8	16
C_{standard}/[MAC]	2.6E3	3.3E5	4.2E7	5.4E9
$C_{\text{efficient}}$/[MAC]	3.0E2	6.0E3	1.5E5	4.5E6
N (with $M=2$ & $K=5$)	2	8	16	32
C_{standard}/[MAC]	2.6E3	1.0E4	2.0E4	4.1E4
$C_{\text{efficient}}$/[MAC]	3.0E2	5.0E2	7.5E3	1.3E3

Tab. 1. Complexity comparison: standard vs. efficient MFB receiver, when $L = 3$.

References

[1] Bluetooth Special Interest Group, *Specification of the Bluetooth System*, February 2002, Core.

[2] Tor Aulin, Nils Rydbeck, and Carl-Erik W. Sundberg, "Continous Phase Modulation-Part II: Partial Response Signaling," *IEEE Transactions on Communications*, vol. COM-29, no. 3, pp. 210–225, March 1981.

[3] Amir Soltanian and Robert E. Van Dyck, "Performance of the Bluetooth System in Fading Dispersive Channels and Interference," in *Proc. Global Telecommunications Conference*, San Antonio, Texas, November 2001, vol. 6, pp. 3499–3503.

[4] Bruce A. Carlson, *Communication Systems*, McGraw-Hill, Singapore, 3rd edition, 1986.

[5] Roel Schiphorst, Fokke Hoeksema, and Kees Slump, "Bluetooth Demodulation Algorithms and their Performance," in *Proc. 2nd Karlsruhe Workshop on Software Radios*, Karlsruhe, March 2002, pp. 99–105.

[6] William P. Osborne and Micheal B. Luntz, "Coherent and Noncoherent Detection of CPFSK," in *IEEE Transactions on Communications*, August 1974, vol. COM-22, pp. 1023–1036.

[7] John B. Anderson, Tor Aulin, and Carl-Erik Sundberg, *Digital Phase Modulation*, Plenum Press, New York and London, 1986.

[8] Charles Tibenderana and Stephan Weiss, "Low-Complexity High-Performance GFSK Receiver With Carrier Frequency Offset Correction," in *Proc. IEEE International Conference on Acoustics, Speech, and Signal Processing*, Montreal, Canada, May 2004, vol. IV, pp. 933–936.

[9] Charles Tibenderana and Stephan Weiss, "Blind Equalisation and Carrier Offset Compensation for Bluetooth Signals," in *European Signal Processing Conference*, Vienna, Austria, September 2004, pp. 909–912.

[10] Raymond Steele and Lajos Hanzo, *Mobile Communications*, John Wiley & Sons, West Sussex, 2nd edition, 1999.

[11] Charles Tibenderana and Stephan Weiss, "A Low-Cost Scalable Matched Filter Bank Receiver for GFSK Signals with Carrier Frequency and Modulation Index Offset Compensation," in *Asilomar Conference on Signals, Systems, and Computers*, Pacific Groove, California, November 2004.

[12] IEEE, New Jersey, *Standard 802.11*, 1999 edition, March 1999.